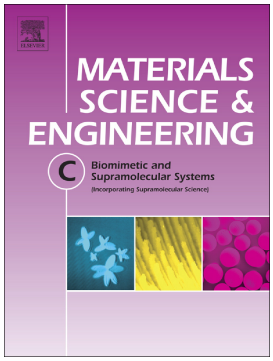

Polythiophene supported MnO2 nanoparticles as nano-stabilizer for simultaneously electrostatically immobilization of d-amino acid oxidase and hemoglobin as efficient bio-nanocomposite in fabrication of dopamine bi-enzyme biosensor

Yalda Shoja, Amir Abbas Rafati, Javad Ghodsi

PII: S0928-4931(16)32046-X
DOI: doi: 10.1016/j.msec.2017.03.155
Reference: MSC 7667

To appear in: *Materials Science & Engineering C*

Received date: 10 November 2016
Revised date: 12 March 2017
Accepted date: 15 March 2017

Please cite this article as: Yalda Shoja, Amir Abbas Rafati, Javad Ghodsi , Polythiophene supported MnO2 nanoparticles as nano-stabilizer for simultaneously electrostatically immobilization of d-amino acid oxidase and hemoglobin as efficient bio-nanocomposite in fabrication of dopamine bi-enzyme biosensor. The address for the corresponding author was captured as affiliation for all authors. Please check if appropriate. Msc(2017), doi: 10.1016/j.msec.2017.03.155

Polythiophene supported MnO_2 nanoparticles as nano-stabilizer for simultaneously electrostatically immobilization of D-amino acid oxidase and hemoglobin as efficient bio-nanocomposite in fabrication of dopamine bi-enzyme biosensor

Yalda Shoja, Amir Abbas Rafati*, Javad Ghodsi

Department of Physical Chemistry, Faculty of Chemistry, Bu-Ali Sina University, P.O.Box 65174, Hamedan, Iran

* To whom correspondence should be addressed

E-mail: **aa_rafati@basu.ac.ir** or **rafati_aa@yahoo.com**

Fax: ++98-81-3838 0709

Abstract

A novel, highly selective and sensitive voltammetric bi-enzyme biosensor for sensing dopamine (DA), in presence of H_2O_2 which resulted as D-alanine enzymatic oxidation, was fabricated on the basis of simultaneously electrostatically immobilization of D-amino acid oxidase (DAAO) and hemoglobin (Hb) on MnO_2 nanoparticles (MnO_2 NPs) enriched poly thiophene (PTh). Cyclic voltammetry (CV), technique was applied for electropolymerization of thiophene on glassy carbon electrode (GCE) surface and MnO_2 NPs dispersed on PTh network by soaking PTh/GCE in potassium permanganate ($KMnO_4$) solution. Excellent catalytic properties and large surface area of MnO_2 NPs/PTh composite caused it was used as an enzymes immobilization host in this developed bi-enzyme biosensor. The developed biosensor was characterized by scanning electron microscopy (SEM), energy dispersive X-ray analysis (EDX), and CV. The performance of the modified bi-enzyme biosensor was investigated in terms of its response time, detection limit, sensitivity, stability and selectivity in a lab environment. The composite of DAAO-Hb/MnO_2 NPs/PTh to construct a bi-enzyme biosensor in this study showed a linear response with DA in the concentration range of 0.04-9.0 µM with R-squared value of 0.994 (for S/N=3) and its sensitivity and detection limite were about 12.801 µA/µM and 41 nM respectively. Also this bi-enzyme biosensors exhibited high selectivity, rapid response (5 s) and long-term stability (42 days). At the end, the proposed biosensor was applied successfully in human serum as real sample.

***Keywords*:** Bi-enzyme biosensor; Dopamine; MnO_2 nanoparticles; D-amino acid oxidase; Hemoglobin; Immobilization

1. Introduction

Enzymes as one kind of significant biomolecules have been widely applied in the detection of various compounds with their catalytic activity and high substrate specificity. In particular, several mono enzymatic biosensors have been reported for dopamine (DA) and some other catechol amines determination by using tyrosinase, [1] laccase [2] and horseradish peroxidase [3, 4] as one of the simplest and most accurate methods. But often traditional DA biosensors have some disadvantages such as low conductivity, low reproducibility, low stability, high over potential, high background currents and high response time in biological fluids. Furthermore, at a high potential, various electroactive compounds, such as ascorbic acid, folic acid and uric acid that are usually present in biological samples can produce unwanted interfering reactions for the detection of the DA. Hence, development of biosensor is still in need for DA measurement in real samples. In recent years, bi-enzyme biosensors have been attached great attentions to overcome these problems. Bi-enzyme biosensors show high selectivity, stability and sensitivity because their low applied potential decreases the noise levels and background currents and eliminates the undesirable oxidation of electroactive interferes species. In these biosensors, peroxidase enzyme, (POx), like horse radish peroxidase, in combination with oxidase enzyme have been studied for the substrate detection in the way of direct or mediated electron transfer [5, 6]. In this regard hemoglobin (Hb), has intrinsic peroxidase like activity commercial availability, structure and relatively higher stability. Therefore it could be an appropriate alternative for horseradish peroxidase, specifically for reducing the fabrication cost and improving the biosensor performance [7, 8]. However, there are only few reports on the measurement of catecholamines or phenolics compounds using Hb-modified biosensors [9, 10].

In order to develop a reusable enzymatic biosensor, reliable immobilization of enzyme is an important point since stability and biological activity of enzyme should be preserved [11-13]. Various nanomaterial have been used for efficient enzymes immobilization on to the electrode surfaces because their extra ordinary properties increases enzyme loading that it can enhance biocatalytic activity of biosensor [14, 15]. Many metal oxides are applied for immobilization of enzymes that among of them MnO_2 nanoparticles have been widely intrested due to their unique properties such as good biocompatibility, high surface/volume ratio, low cost, strong electrocatalytic activity, high energy density and high conductivity [16-19]. On the other hand, conductive polymers have ability to effectively transfer electric charge produced by the biochemical reactions to electronic circuit in biosensors [20]. Polythiophene (PTh) is one type of the most interested conducting polymers which are useful in many applications such as solar cells, sensors, biosensors, organic field effect transistor, super capacitors, light emitting diodes and electrochromic devices [21]. Recently, the composite containing conductive polymers and MnO_2 are paid more consideration for construction various electrodes because of their excellent stability, high conductivity and good mechanical flexibility [22, 23].

In this work , for the first time, DA was measured by using D-alanine enzymatic catalized oxidation. Indeed Hb was applied as electrocatalyst for DA oxidation in presence of H_2O_2 which was in situ generated by D-amino acid oxidase, (DAAO)-catalyzed oxidation of D-alanin, while in most oxidase/peroxidase bi-enzyme biosensor POx (herein Hb), catalyzes the H_2O_2 response. Dopamine, (DA), is belonged to catecholamine neurotransmitters which are an important group of biogenic compounds that are mediators in transmitting messages between neurons [24]. It has proved that changes in DA levels to be important in efficient brain functions for example dopamine deficiency results in Parkinson's disease and people with low dopamine activity may

be more prone to addiction [25]. On the other hand D-amino acids (DAAs) have an important role in life science since several DAAs are found to have physiological functions in mammals [26]. For example D-alanine in the gland, anterior pituitary, plasma and pancreas might have a physiological function to the insulin regulation [27-30]. Thus it can be said measurement of DA in presence of DAAs like D-alanine is possible and necessary.

For this purpose, PTh electropolymerized on glassy carbon electrode (GCE) surface by applying cyclic voltammetry and MnO_2 nanoparticles dispersed on to PTh/GCE by directly soaking PTh/GCE into a potassium permanganate solution. Then Hb and DAAO were electrostatically immobilized on MnO_2 nanoparticles. The enzymes were positively charged and could assemble with negatively charged MnO_2 nanoparticles by electrostatic interaction. Hb could catalyze the oxidation of DA and avoid the interferences. As far as we know, MnO_2 nanoparticles/PTh nanocomposite was used in fabrication of biosensor for the first time in this study but it has various applications in other electrochemical fields. For example MnO_x/PEDOT/MWCNTs nanocomposite was used as catalyst support for Pt nanoparticles in methanol electrooxidation.[31]. Finally the prepared biosensor was characterized with the methodologies as SEM, Energy dispersive X-ray spectroscopy (EDS) and CV and its performance in human serum was investigated.

2. Experimental

2.1. Chemicals and reagents

Dopamine (DA), folic acid (FA), uric acid (UA) and ascorbic acid (AA) were obtained from darou pakhsh.co (Iran). DAAO (EC 1.4.3.6, DAAO) was from porcine kidney (1.5 units mg^{-1} of solid), D-alanine, Hb and tetrabutylammonium perchlorate (TBAPC), were purchased

from Sigma-Aldrich. Thiophene was from Merck. All other reagents were of analytical grade and used without further purification. All electrochemical measurements were performed at 50 mM in a phosphate buffer (PB) of pH 6.0 and all experiments were carried out at room temperature (25 ± 0.1 °C).

2.2. Apparatus

Electrochemical measurements were carried out with a computer-controlled μ-Auto lab modular electrochemical system (PGSTAT101, the Netherlands), driven with NOVA Software (upgrade 1.10). A conventional electrochemical 3 electrode system was used for all electrochemical experiments with an Ag/AgCl electrode (saturated potassium chloride), a GC (diameter 2 mm) electrode and a Pt foil as reference, work and counter electrodes respectively. EDS and SEM images were obtained using a VEGA TESCAN SEM. All solutions were deoxygenated with pure nitrogen for at least 5 min.

2.3. Procedures

2.3.1 Modification of glassy carbon electrode with polythiophene (PTh/GCE)

CV was applied for electropolymerization of thiophene at GCE surface in deaerated acetonitrile solution containing 0.01 M TBAPC and 5×10^{-3} M thiophene monomer to prepare PTh/GCE. The electrode potential was cycled between 0.0 and 1.7 V at a scan rate of 50 mVs^{-1} for 20 cycles in a cyclic voltammetry regime. After electropolymerization, the PTh/GCE was kept at a reducing potential (−0.2 V) for 10 min to undope from the original electrolyte anion. Solution was bubbled with N_2 for 5 min before electropolymerization.

2.3.2 Preparation of MnO_2 NPs/PTh composite GCE

The dispersion and formation of MnO_2 nanoparticles on PTh/GCE were carried out according previous literature [32]. In detail, PTh/GCE was soaked in 10 mM potassium permanganate solution for10 min. MnO_2 nanoparticles grew in the PTh/GCE surface during this soaking process. The obtained electrode washed with PBS and dried at room temperature. Scheme 1 shows the possible oxidation mechanism of the thiophene sulfur into sulfoxide by $KMnO_4$.

2.3.3 Fabrication of DAAO-Hb/MnO_2 NPs/PTh/GCE bi-enzyme biosensor

The DAA-Hb/MnO_2 NPs/PTh/GCE was prepared by dipping of MnO_2 NPs/PTh/GCE in to solution, which was containing DAAO and Hb in PBS (100 mM, pH =6). As expected from isoelectric points of DAAO, Hb and MnO_2 the DAAO and Hb electrostatically were immobilized onto the surface of MnO_2/ PTh/GCE. Isoelectric points of DAAO,Hb and MnO_2 NPs are about 7.0, 7.0 and 4.5, respectively [9, 33, 34]; so, in the pH = 6, positively charged DAAO and Hb can immobilize onto the negatively charged MnO_2 NPs. Optimized experimental parameters including dipping time, pH, DAAO and Hb concentration for maximum DAAO and Hb immobilization were obtained and applied for the next preparation of bi-enzyme biosensor. The amount of immobilized DAAO and Hb on MnO_2 NPs was investigated from the difference in UV-Vis absorbance of DAAO and Hb solution in about 280 nm before and after treating with MnO_2 NPs. UV-Vis absorbance of DAAO and Hb was related to DAAO and Hb concentration by applying a standard calibration curve for them (obtained as milligrams per milliliter of DAAO and Hb vs. UV-Vis absorbance at ~ 280 nm).Finally the obtained bi-enzyme biosensor washed with PBS buffer of pH =6 to remove the unimmobilized DAAO and Hb. Fabrication steps of biosensor is shown in scheme 2.

3. Results and discussion

3.1. Electropolymerization of PTh at GCE and characterization of DAA-Hb/MnO_2 NPs/PTh/GCE bi-enzyme biosensor

The consecutive CVs corresponding to the electropolymerization of thiophene on GCE surface is presented in Fig 1. As it can be seen, there is a successive increase of current during continuous cycling implying the growth of the PTh film at the GCE surface [35]. Figs. 2a and 2b show the SEM images of PTh/GCE and MnO_2 NPs/PTh/GCE respectively. The stepwise modification of GCE by DAAO-Hb/MnO_2 NP/PTh composite could be seen clearly from these SEM images. The SEM image of PTh/GCE confirms the formation of a film layer of polymer on GCE surface. Fig. 2b is the SEM image of $KMnO_4$ treated PTh network on GCE surface. As can be seen in this figure, dispersed MnO_2 NPs on to PTh/GCE surface have uniform distribution in the range 47-60 nm in diameter. This high surface/volume ratio provided high surface area for enzymes immobilization and also improved performance of biosensor. significant experimental parameters including dipping time, pH, DAAO and Hb concentration that affect DAAO and Hb immobilization on MnO_2 NPs were evaluated, and the optimized parameters were determined. The optimized dipping time and DAAO and Hb concentration for maximum immobilization were determined to be about 30 min and 10 mg/10 ml of each DAAO and Hb, respectively. As expected, the optimized pH obtained was about 6 which is approximately between that of MnO_2 and DAAO and Hb isoelectric points. Fig. 2c exhibits the EDX spectrum of DAAO-Hb/MnO_2 NPs/PTh/GCE. As expected, this figure revealed that the surface of modified bi-enzyme biosensor contained C, N, Fe, Mn, S and O elements with 40.18, 18.83, 2.05, 10.72, 14.89 and 13.33 Wt.%, respectively. Emerging of Mn, S, N and Fe element peaks in modified biosensor

EDX analysis by DAAO-Hb/MnO_2 NPs/PTh composite, clearly refers to MnO_2 NPs dispersed on PTh matrix, DAAO and hem group of Hb which successfully immobilized on MnO_2 NPs. Finally Fig. 3 shows the FT-IR spectra of DAAO-Hb/MnO_2 NPs. The bands observed at about 600 cm^{-1} is attributed to the characteristic stretching collision of O–Mn–O, which verified the presence of the MnO_2 in the sample [36]. Characteristic DAAO and Hb peaks at about 1650, 1630 and 1533 cm^{-1} in FT-IR spectrum are corresponded to the amide I, amide II, and C-N stretching modes, respectively [9, 37] that strongly demonstrated the attachment of DAAO and Hb molecules onto MnO_2 NPs. Also typical characteristic PTh peaks at 1043, 1071, 1216 and 1433 cm^{-1} in FT-IR spectrum are assigned to the stretching vibration of C-H out-of-plane, C-S, in-plane C-H and C-C stretching vibratin respectively [38].

3.2. Electrochemical investigations of the MnO_2 NPs/PTh/GCE

The comparison between bare GCE, PTh/GCE and modified GCE by MnO_2 NPs/PTh composite was done by electrochemical investigation of these electrodes. For electrochemical study, the CVs of bare GCE, PTh/GCE and MnO_2 NPs/PTh/GCE were measured in 0.1 M KNO_3 solution containing 5.0 mM $K_3[Fe(CN)_6]$. As it is shown in Fig. 4, potential peak separations for $[Fe(CN)_6]^{3-}$/$[Fe(CN)_6]^{4-}$ redox were about 359.5 mV, 224.6 mV and 168.5 mV at bare GCE, PTh/GCE and MnO_2 NPs/PTh/GCE surface respectively. The smaller peak separation indicates more reversible one electron transfer reaction and also significantly larger electron transfer rate for modified GCE rather than bare GCE. It can be said, the peak current and reversibility of $[Fe(CN)_6]^{3-}$/$[Fe(CN)_6]^{4-}$ increased after electropolymerization of PTh on GCE because of electrostatic attraction between positive charge of PTh and negative charge of $[Fe(CN)_6]^{3-/4-}$. When MnO_2 NPs were assembled on the surface of PTh/GCE, the peak current of [Fe

$(CN)_6]^{3-}$/[Fe $(CN)_6]^{4-}$ redox significantly increased that was due to good electrocatalytic ability of the MnO_2 NPs/PTh composites. On the other hand, effective surface area is another important electrochemical parameter of electrode that is related to peak height. As can be seen in Fig. 4, the MnO_2 NPs/PTh/GCE peak current is higher than bare GCE peak current that implies a larger effective surface area for modified GCE. The effective surface area was calculated from Randles-Sevcik equation (at 25 °C) [39]:

$$i_p = (2.69 \times 10^5)\, n^{3/2}\, ACD^{1/2}\, \nu^{1/2} \quad (1)$$

where i_p is the peak current for a reversible redox couple at 25 ºC, A is effective surface area (in cm^2), n is the number of electrons transferred, D is the diffusion coefficient (that is 7.35×10^{-6} cm^2 s^{-1} for 1 mM of $[Fe(CN)_6]^{-4}$ [40]), ν is the scan rate (in V/s) and C is the bulk concentration (in mol cm^{-3}). According to Eq. 1, the peak current increases with square root of the scan rate and is directly proportional to concentration. Therefore CV voltammograms at a series of scan rates ranging from 10 to 300 mV/s in 0.1 M of KCl solution containing 5.0 mM $K_3[Fe(CN)_6]$ for bare GCE (Fig. 5a), and the MnO_2 NP/PTh/GCE (Fig. 5b) were measured. The electrode effective surface area calculated about 0.015 cm^2 and 0.03 cm^2 for bare GCE and modified GCE, respectively from the slope of anodic peak current versus square root of scan rates (Fig. 5c). These results verify larger effective surface area for MnO_2 NPs/PTh/GCE. Also it is observable from Fig. 5c that the anodic peak currents increase in a linear relationship with the square root of scan rates for MnO_2 NPs/PTh/GCE which demonstrates the process of [Fe $(CN)_6]^{3-}$/[Fe $(CN)_6]^{4-}$ redox is mainly diffusion controlled. To furthermore electrochemical investigation, Fig. 5d shows the peak potentials, extracted from the CVs in Figs. 4a and 4b, were plotted versus scan rate. As can be seen in this figure, for bare GCE with increasing of scan rate, the peak separation increased significantly, which is related to low electron transfer rate for this

electrode. In comparison with bare GCE, the peak separation for modified GCE remains constant with increasing scan rate, which indicates the high electron transfer rate for this electrode. Accordingly, the MnO_2 NPs/PTh/GCE shows (1) larger effective surface area and (2) higher electron transfer rate rather than the bare GCE that is due to nano dimension and electrocatalytic activity of MnO_2 NPs/PTh composite.

3.3. Electrochemical characterization of DAAO-Hb/MnO_2 NPs/PTh/GCE bi-enzyme biosensor

The CVs of three different modified electrodes in PBS (100 mM, pH = 6.0) at a scan rate of 100 mV s^{-1} were showed in Fig. 6. CVs of a, b and c are corresponded to bare GCE, MnO_2 NPs/PTh/GCE and DAA-Hb/MnO_2 NPs/PTh/GCE respectively. As shown, no redox peak appears for all of the three electrodes. Therefore, it can be concluded that no any direct electron transfer was happened between the DAAO, Hb and MnO_2 NPs with each other and also with the electrode surface.

3.4. Biosensing of H_2O_2 and electrocatalytical behavior of the DAAO-Hb/MnO_2 NP/PTh/GCE bi-enzyme biosensor in the presence of H_2O_2

In most of the bi-enzyme biosensors, peroxidases or hemoglobin acts as mediator for electron transferring between H_2O_2 resulted from oxidase enzyme reaction with its substrate and electrode surface. While in this work, Hb acts as electrocatalyst for dopamine oxidation and not as mediator. Hb should be activated with H_2O_2 to perform its electrocatalyst role. H_2O_2 requisite for Hb activating is supplied from D-alanine oxidation by DAAO. In this work dopamine as phenolic compound was measured by peroxidase properties of Hb in presence of a fixed amount of D-alanine.

Fig. 7 shows CV voltammograms of bare GCE and DAAO/MnO_2 NPs/PTh/GCE in PBS (100mM, pH=6), in presence of 200 µM D-alanine. As can be seen, there is no reduction peak at the bare GCE in presence of D-alanine, (curve a). In contrast, DAAO/MnO_2 NPs/GCE shows remarkable response current toward reduction of H_2O_2 at -0.53 V [41] which was produced from D-alanine oxidation by DAAO, in comparison with bare GCE. In next step, Hb in DAAO-Hb/MnO_2 NPs/PTh/GCE biosensor is oxidized by H_2O_2. Electrocatalytic behavior of the bi-enzyme biosensor was investigated by CV measurment. No redox peak of Hb and DAAO that electrostatically immobilized on MnO_2 NPs/PTh/GCE in 100mM PBS (pH= 6.0) was appeared. It can be said there is no direct electron transfer between the oxidized form of Hb and the GCE surface. The CV voltammogram of this experiment is similar to CV voltammogram of DAA/Hb/MnO_2 NPs/GCE in absence of D-alanine (Fig. 6 curve c).

3.5. Bioelectrocatalytic oxidation of dopamine in presence of D-alanine at the bi-enzyme-based biosensor

Electrocatalytic response of the bi-enzyme biosensor was characterized by CV measuements. Fig. 8 shows the CV voltammograms of four differently modified GCE in 100mM PBS (pH = 6.0) containing fix amount of D-alanine (200 µM) and DA (5 µM). As can be concluded from this figure, no electrocatalytic reduction or oxidation peak was observed at bare GCE, PTh/GCE and MnO_2 NPs//PTh/GCE surface (curve a, b and c respectively). The redox peak current corresponding to DA by DAAO-Hb/MnO_2 NPs/PTh/GCE were appeared at around 0.17 V for anodic peak and 0.11 V for cathodic peak respectively (curve d). It can be said this modified bi-enzyme biosensor exhibits high electrocatalytic activity for oxidation of DA which is related to the simultaneous presence of Hb as electrocatalyst and MnO_2 NPs/PTh composite in

this modified GCE. MnO_2 NPs/PTh composite not only is used as nano-stabilizer for enzymes immobilization in developed bi-enzyme biosensor, but also increases the electrode surface area due to a well-organized packaging of PTh film that electropolymerized on GCE surface and high surface/volume ratio of MnO_2 NPs dispersed on PTh film. Oxidation mechanism of DA by proposed bi-enzyme biosensor is shown in scheme 3. As it is seen from this scheme, in first step, the oxidation of D-alanine to α-ketoacid and production of H_2O_2 was catalyzed by DAAO. This may suggest the catalytic role of hem of Hb in dopamine oxidation as follows: in this electrode, hem of Hb was oxidized by H_2O_2 present in the solution, In second step, oxidized hem could easily oxidize the dopamine (or other phenolic compounds) on the electrode surface. Finally, electron transferrence from hem to the electrode caused anoxidation peak current that was directly dependent on the dopamine In second step level in the sample. In fact, hem acts as a mediator for electron transfer from dopamine to electrode.

3.6 Effect of the potential scan rate on biosensor performance

Fig. 9a displays the CV voltammograms of the DAAO-Hb/MnO_2 NPs/PTh/GCE at different scan rates for 5 µM DA in PBS 100 mM (pH = 6.0) containing 200 µM D-alanine for kinetic investigation of electrode reaction. Fig. 9b exhibits a linear relationship between anodic and cathodic peak current *vs.* square root of scan rate in ranges of 10-900 mV/s by R^2 values of about 0.995 and 0.985 respectively. This result indicates that the bioelectrochemical oxidation of DA on modified bi-enzyme biosensor is diffusion controlled current.

3.7 Calibration curve for determination of dopamine and detection limit of the bi-enzyme biosensor

Determination of DA was carried out by using differential pulse voltammetry (DPV), method. Fig. 10a represents DPV voltammograms of DA obtained by modified bi-enzyme biosensor by successive additions of DA to 100 mM of PBS (pH = 6.0) containing 200 µM D-alanine. Fig. 10b shows the respective calibration curve of DAAO-Hb/MnO_2 NP/PTh/GCE with correlation coefficients of 0.994. According to this results the modified biosensor has the detection limit of 41 nM (at S/N of 3) in linear range concentration of 0.04-9.0 µM, a rapid current response time (within 5 s) to DA and possess the sensitivity of 12.801 µA μM^{-1}. The good linear responce to the DA concentration (R^2= 0.994), an excellent linear range, high sensitivity, low detection limit and high stability modification process suggest that the developed bi-enzyme biosensor in this study can be comparable or even better than other previously reported works. Table 1 shows a comparison between performance of some previously reported voltammetric and amperometric methods and our proposed modified bi-enzyme biosensor in this work for the determination of DA. The biological activity of immobilized enzyme was evaluated by the apparent Michaelis–Menten constant (K_m) that can be calculated from the Lineweaver–Burk equation for the basic Michaelis–Menten equation:

$$\frac{1}{V} = \left(1 + \frac{K_m}{[S]}\right)\frac{1}{V_{max}} \quad (2)$$

In electrochemical methods, the Lineweaver–Burk equation is:

$$\frac{1}{I} = \left(1 + \frac{K_m}{[S]}\right)\frac{1}{I_{max}} \quad (3)$$

Where peak current (I) is a criterion for reaction rate in this equation, K_m is Michaelis–Menten constant and [S] is substrate concentration [45]. Fig. 9c depicts Lineweaver-Burk plot of the DAAO-Hb/MnO_2 NPs/PTh/GCE at different DA concentration in range of 0.2 to 0.5 μM (obtained from calibration curve). Smaller Michaelis–Menten constant shows the high activity of enzyme. K_m was obtained about 0.98 μM for modified bi-enzyme biosensor which is much less than that those of Hb in AuNPs-carbon aerogel and ionic liquid film of 0.48 mM [46], Hb immobilized on carbon nanochips film of 21.55 μM [47], Hb immobilized on Pd@Fe3O4-MWCNTnanocomposite of 21.55 μM [48] and Hb on graphene-copper sulfide nanocomposite of 6.3 mM [49]. Therefore this result verifies the modified bi-enzyme biosensor possesses higher biological sensitivity toward DA.

3.8 Selectivity, stability and repeatability

The selectivity of the proposed bi-enzyme biosensor was examined by studying the interfering effects of relevant electroactive species such as ascorbic acid, folic acid and uric acid with the CV measurment of DA. It was observed that the effect of the interfering species on the DA detection is negligible, which confirmed high selectivity and sensitivity of the fabricated bi-enzyme biosensor toward dopamine oxidation. The stability of bi-enzyme biosensor was evaluated by investigation of the biosensor response for a period of 42 days under its storage at 4 °C in PBS 100 mM (pH = 6.0). Biosensor retains 75% of maximum initial current response at the first day of fabrication after 4 weeks and at the end the current response of the biosensor decreased to 60% of its primary response after 6 weeks. Therefore, these observations confirm the good stability of bi-enzyme biosensor. Also, this bi-enzyme biosensor exhibits approximately a same response after 12 successive determinations of a constant amount of DA in in PBS 100

mM (pH = 6.0) . Relative standard deviations (RSD) 2.95% was obtained that indicates the fabricated biosensor has a good repeatability.

3.9 Real sample analysis

The developed bi-enzyme biosensor was successfully used to determine DA in human serum as real sample. The human serum sample was centrifuged then it was diluted 40 times with PBS 100 mM (pH = 6.0). The standard addition method was applied for quantitative analysis of DA. The relative recovery percentage (RR %) in Table 2 is defined as following equation [50]:

$$\text{Recovery (\%)} = (C_{found} - C_{real}/C_{added}) \times 100 \qquad (4)$$

Where $C_{added,}$ C_{found} and C_{real} are the concentration of known amount of standard which was spiked to the real sample, the concentrations of analyte after addition of known amount of standard in the real sample and the concentration of analyte in real sample, respectively. The results revealed average recovery was about 97.5 % for DA which added to human serum samples (Table 2). Therefore it can be concluded, according to these results, this modified bi-enzyme biosensor provides a reliable and applicable method for the determination of DA in biological samples.

4. Conclusion

Summarily in this work, we described a bi-enzyme biosensor for DA sensing base on electrostatically immobilization of DAAO and Hb on MnO_2 NPs/PTh network modified GCE. PTh was electropolymerized on GCE surface and MnO_2 NPs loaded on PTh by soaking the PTh network in $KMnO_4$ solution. The fabricated bi-enzyme was characterized by SEM, EDX and

CV. The experimental results showed excellent characteristics for detection and measurement of DA such as good linear range (R^2 = 0.994), low detection limit (41 nM), high sensitivity (12.801 µA/µM), rapid response time (5 s), good storage stability (42 days) and an average recovery of 97.5% in human serum samples. These results confirmed an efficient catalytic property of GCE modified with DAAO-Hb/MnO_2 NPs/PTh composite for detection and determination of DA that could offer a reliable bi-enzyme biosensor for other phenolic compounds.

References

[1] C. Lete, S. Lupu, B. Lakard, J.Y. Hihn, F. J. del Campo, J. Electronal. Chem. 744 (2015) 53–61.

[2] Z. Hua, Q. Qin, X. Bai, C. Wang, X. Huang, Sens. Actuators B 220 (2015) 1169–1177.

[3] P. Raghu, T.M. Reddy, P. Gopal, K. Reddaiah, N.Y. Sreedhar, Enzyme. Microb. Technol. 57 (2014) 8–15.

[4] Y. Shoja, A.A. Rafati, J. Ghodsi, Mater. Sci. Eng. C 58 (2016) 835–845.

[5] H. Chen, C. Mousty, L. Chen, S. Cosnier, Mater. Sci. Eng. C 28 (2008) 726-730.

[6] Y. Fang, Y. Umasankar, R. P. Ramasamy, Biosens. Bioelectron. 81 (2016) 39–45.

[7] S. Palanisamy, S. Cheemalapati, S.M. Chen, Anal. Biochem. 429 (2012) 108–115.

[8] A. Hajian J. Ghodsi, A. Afraz, O. Yurchenko, G. Urban, Mater. Sci. Eng. C 69 (2016) 122-127.

[9] J. Ghodsi, A.A. Rafati, Y. Shoja, M. Najafi, J. Electrochem. Soc. 162 (2015) B69–B74.

[10] A.K.M. Kafi, D.Y. Lee, S.H. Park, Y.S. Kwon, Thin Solid Films. 516 (2008) 2816–21.

[11] B. Kowalewska, K. Jakubow, Sens. Actuators B 238 (2017) 852-861.

[12] Y. Guan, L. Liu, C. Chen, X. Kang, Q. Xie, Talanta 160 (2016) 125-132. Mater. Sci. Eng. C 71 (2017) 75-83.

[13] X. Cai, X. Gao, L. Wang, Q. Wu, X. Lin, Sens. Actuators B 181 (2013) 575– 583.

[14] J. Huang, H. Liu, P. Zhang, P. Zhang, M. Li, L. Ding, Mater. Sci. Eng. C 57 (2015) 31-37.

[15] E. Cherian, M. Dharmendirakumar, G. Baskar, Chinese J. Catal. 36 (2015) 1223–1229.

[16] Y. Pan, Z. Hou, W. Yi, W. Zhu, F. Zeng , Y.N. Liu, Talanta 141 (2015) 86–91.

[17] J. Lu, X. Zhang, X. Zhang, N. Liu, H. Li, Z. Yu, X. Yan, Electrochim. Acta 174 (2015) 221–229.

[18] S.R. Srither, A. Karthik, S. Arunmetha, D. Murugesan, V. Rajendran, Mater. Chem. Phys. 183 (2016) 375-382.

[19] Z. Hu, Y. Zhao, J. Liu, J. Wang, B. Zhang, X. Xiang, J. Colloid Interface Sci. 483 (2016) 26-33.

[20] T. Ahuja, I.A. Mir, D. Kumar, Rajesh, Biomaterials 28 (2007) 791–805.

[21] A. Hajian, A.A. Rafati, A. Afraz, M. Najafi, J. Electrochem. Soc. 161 (2014) B196-B200.

[22] P. Tang, Y. Zhao, C. Xu, Electrochim. Acta 89 (2013) 300– 309.

[23] B. Babakhani, D.G. Ivey, Electrochim. Acta 55 (2010) 4014-4024.

[24] T. Łuczak, Electroanalysis 20 (2008) 1639 – 1646.

[25] T. Yin, W. Wei, J. Zeng, Anal. Bioanal. Chem. 386 (2006) 2087–2094.

[26] C. H. Nieh, Y. Kitazumi,O. Shirai, K. Kano, Biosens. Bioelectron. 47 (2013) 350–355.

[27] K. Hamase, A. Morikawa, S. Etoh, Y. Tojo, Y. Miyoshi, K. Zaitsu, Anal. Sci. 25 (2009) 961–968.

[28] Q. Xia, Y. Huang, X. Lin, S. Zhu, Y. Fu, Biochem. Eng. J. 113 (2016) 1-6.

[29] M. Wcislo, D. Compagnone, M. Trojanowicz, Bioelectrochemistry 71 (2007) 91–98.

[30] Z.M. Zain, R.D. O'Neill, J.P. Lowry, K.W. Pierce, M. Tricklebank, A. Dewa, S. Ab Ghani, Biosens. Bioelectron. 25 (2010) 1454–1459.

[31] L. Wei, Y.J. Fan, J.H. Ma, L.H. Tao, R.X. Wang, J.P. Zhong, H. Wang, J. Power Sources 238 (2013) 157-164.

[32] Ran Liu, Jonathon Duay, Sang Bok Lee, ACS Nano. 4 (2010) 4299–4307.

[33] K. Yagi, N. Ohishi, J Biochem, 71 (1972) 993-998.

[34] S.F. Chin, S.C. Pang, M.A. Anderson, Mater. Lett. 64 (2010) 2670-2672.

[35] D. Bouchta, N. Izaoumen, H. Zejli, M. El Kaoutit, K.R. Temsamani, Biosens. Bioelectron. 20 (2005) 2228–2235.

[36] Y.J Huang, W.S. Li, J. Inorg. Mater. 28 (2013) 341-346.

[37] J. Ghodsi, A. Rafati, Y. Shoja, Anal. Bioanal. Chem. 408 (2016) 3899-3909.

[38] R. C. Liu, Z. P. Liu, Chin. Sci. Bull. 54 (2009) 2028-2032.

[39] Y. Shoja, A.A. Rafati, J. Ghodsi, Electrochim. Acta 203 (2016) 281-291.

[40] D. R. Lide, CRC Handbook of Chemistry and Physics, 85 th Edition, CRC PressI Llc, 2004.

[41] A. Afraz, A.A. Rafati, A. Hajian, J. Solid State Electrochem. 17 (2013) 2017–2025.

[42] A. Roychoudhury, S. Basu, S.K. Jha, Biosens. Bioelectron. 84 (2016) 72-81.

[43] H.L. Zou, B. L. Li, H. Q. Luo, N. B. Li, Sensors Actuators B Chem. 207 (2015) 535–541.

[44] K. Wang, P. Liu, Y. Ye, J. Li, W. Zhao, X. Huang, Sens. Actuators B 197 (2014) 292–299.

[45] F.R. Shu, G.S. Wilson, Anal. Chem. 48 (1976) 1679–1686.

[46] S. George, H.K. Lee, J. Phys. Chem. B 113 (2009) 15445–15454.

[47] L. Peng, S. Dong, N. Li, G. Suo, T. Huang, Sens. Actuators B 210 (2015) 418–424.

[48] M. Baghayeri, H. Veisi, Biosens. Bioelectron. 74 (2015) 190–198.

[49] F. Shi, W. Zheng, W. Wang, F. Hou, B. Lei, Z. Sun, W. Sun, Biosens.Bioelectron. 64 (2015) 131–137.

[50] M. Behbahani, F. Najafi, S. Bagheri, M. Kalate Bojdi, P. Ghareh Hassanlou, A. Bagheri, Environ. Monit. Assess., 186 (2014) 2609-2618.

Table 1. Comparison between of our developed bi-enzyme biosensor performance for determination of DA with some various methods previously reported.

Methods/Materials	Linear range	Detection limit	Sensitivity (µA/µM)	stability	Ref.
CV/Tyrosinase/NiO/ITO	2-100 µM	1.04 µM	0.06 µA/mM	45 days	[42]
DPV/Hemin functionalized graphene oxide sheets	0.5 to 40 µM	0.17 µM	0.04623µA/µM	12 days	[43]
CV/SPE/rGO-CDBA-Lac	0.1–70 µM	0.03 µM	0.1041µA /µM	1 month	[2]
CV/Lac/SiO_2-PA/GCE	0.99–103.10 µM	0.26 µM	0.0015 µA/µM	20 days	[44]
DPV/ DAAO-Hb/MnO_2 NPs/PTh/GCE	0.01 to 2.25 µM	41 nM	12.801 µA/µM	42 days	This work

Table 2. Results of the recovery analysis of DA spiked in human serum samples.

Spiked (µM)	Found (µM)	Recovery %	Uncertainty %
0.5	0.45	90	─ 10 %
1.0	1.1	110	+ 10 %
2.0	1.85	92.5	─ 7.5 %

Figures captions:

Scheme 1. Reduction mechanism of $KMnO_4$ by PTh to form MnO_2.

Scheme 2. Fabrication steps of the DAAO-Hb/MnO_2 NPs/PTh/GCE bi-enzyme biosensor.

Scheme 3. Oxidation mechanism of DA by DAAO-Hb/MnO_2 NPs/PTh/GCE bi-enzyme biosensor.

Figure 1. Consecutive cyclic voltammograms for the electropolymerization of thiophene at GCE surface in acetonitrile solution containing 0.01 M TBAPC and 5×10^{-3} M thiophene monomer to prepare PTh/GCE at a scan rate of 50 mV/s. The voltammograms represent 20 sweep segments from 0.0 to 1.7 V at 0 °C.

Figure 2. SEM images of (a) PT/GCE, (b) MnO_2 NPs/PTh/GCE and (c) EDX spectrums analysis of DAAO-Hb/MnO_2 NPs/PTh/GCE with %wt of presence elements.

Figure 3. FT-IR spectrum of DAAO-Hb/MnO_2 NPs.

Figure 4. CVs of (a) bare GCE, (b) PTh/GCE and (c) MnO_2 NPs/PTh/GCE in 0.1M KCl solution containing 5.0 mM $K_3[Fe(CN)_6]$ at a scan rate of 100 mV/s.

Figure 5. (a) CVs of bare GCE at different scan rates (curves A–M: 10, 20, 30, 40, 50, 60, 70, 80, 90, 100, 150, 200, 250 and 300 mV/s), (b) CVs of MnO_2 NPs/PTh/GCE at different scan rates (curves Ã–Ñ: 10, 20, 30, 40, 50, 60, 70, 80, 90, 100, 150, 200, and 300 mV/s), (c) The fitted I_{pa} versus the square root of the scan rates and (d) The cathodic and anodic peak potentials versus the scan rates. All in 0.1M KCl solution containing 5.0 mM $K_3[Fe\ (CN)_6]$.

Figure 6. CVs of (a) bare GCE, (b) MnO_2 NP/PTh/GCE and (c) DAA-Hb/MnO_2 NPs/PTh/GCE in pure PBS solution (100 mM, pH=6) at scan rate of 100 mV/s.

Figure 7. Shows CV voltammograms of (a) bare GCE and (b) DAAO/MnO_2 NPs/PTh/GCE in PBS (100 mM, pH=6) containing of 200 µM D-alanine at scan rate of 100 mV/s.

Figure 8. CVs of (a) bare GCE, (b) PT/GCE, (c) MnO_2 NPs/PTh/GCE and (d) DAAO-Hb/MnO_2 NPs/PTh/GCE in PBS solution (100mM, pH=6) containing 200 µM D-alanine and 5 µM DA at scan rate of 100 mV/s.

Figure 9. CVs of (a) DAAO-Hb/MnO_2 NPs/PTh/GCE in PBS (100mM, pH=6.0) containing 5 µM DA at different scan rates (from A–M) :10, 20, 30, 40, 50, 70, 100, 200, 300,

400, 500, 700 and 900 mV/s) and (b) dependence of anodic and cathodic peak currents vs. square root of scan rate.

Figure 10. DPVs of (a) DAAO-Hb/MnO_2 NPs/PTh/GCE in PBS (100 mM, pH = 6.0) containing 200 µM D-alanine upon increasing the concentration of DA. A-Vcorrespond to 0.04, 0.8, 1.2, 1.6, 2.0, 2.4, 2.8, 3.2, 3.6, 4.0, 4.4, 4.8, 5.2, 5.6, 6.0, 6.4, 6.8, 7.2, 8.0, 8.4, 8.8, and 9.0 µM of DA and (b) calibration curve obtained from DPVs voltammograms data for DA in range 0.04-9.0 µM and (c) Lineweaver-Burk curve for DA determination with the modified biosensor obtained from calibration curve at scan rate of 50 mV/s.

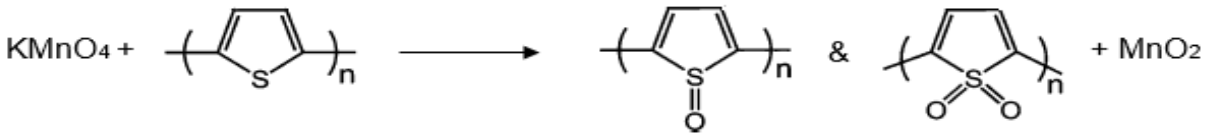

Scheme 1

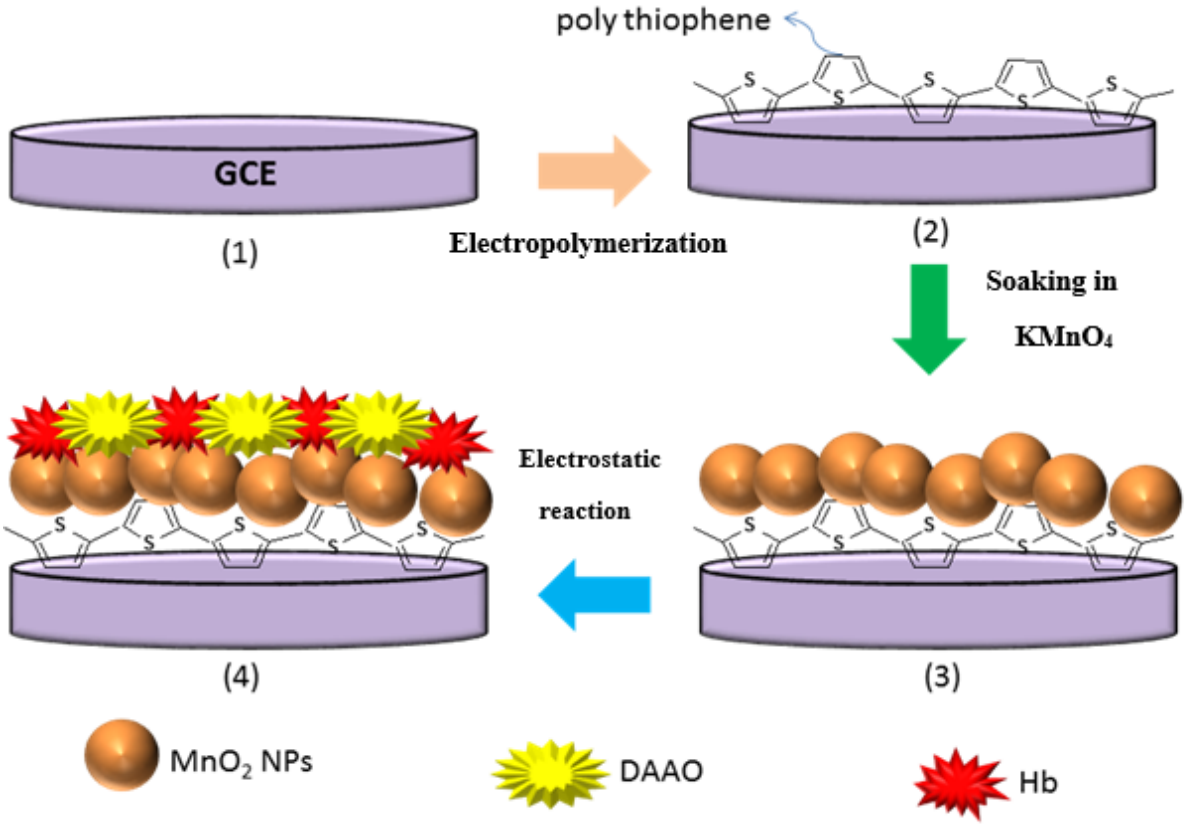

Scheme 2

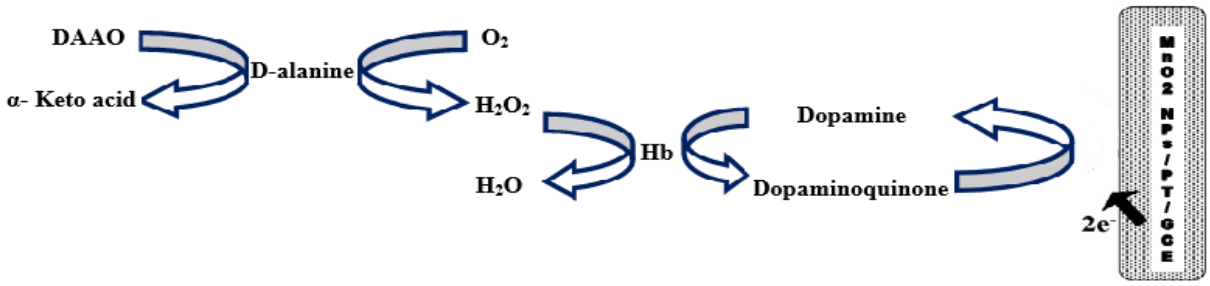

Scheme 3

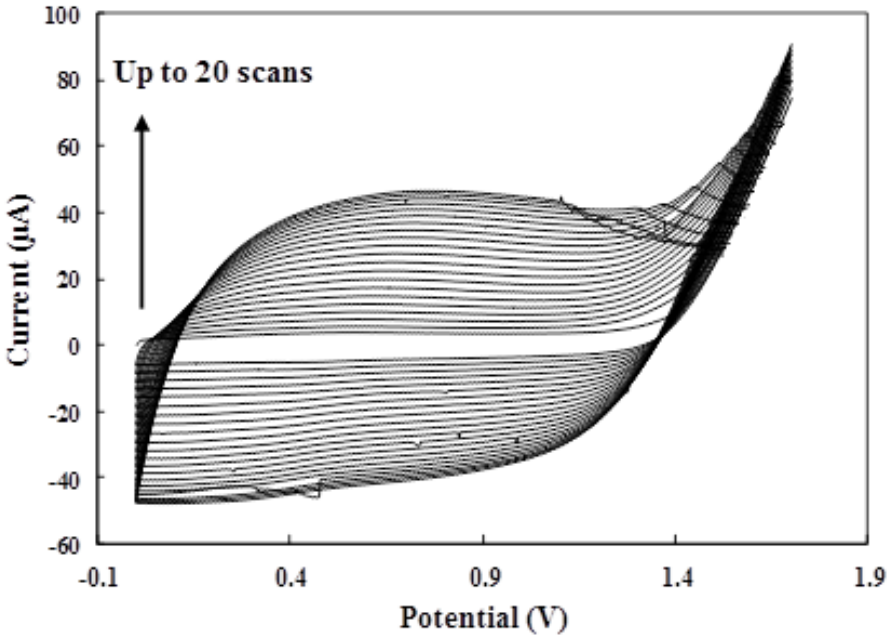

Figure 1

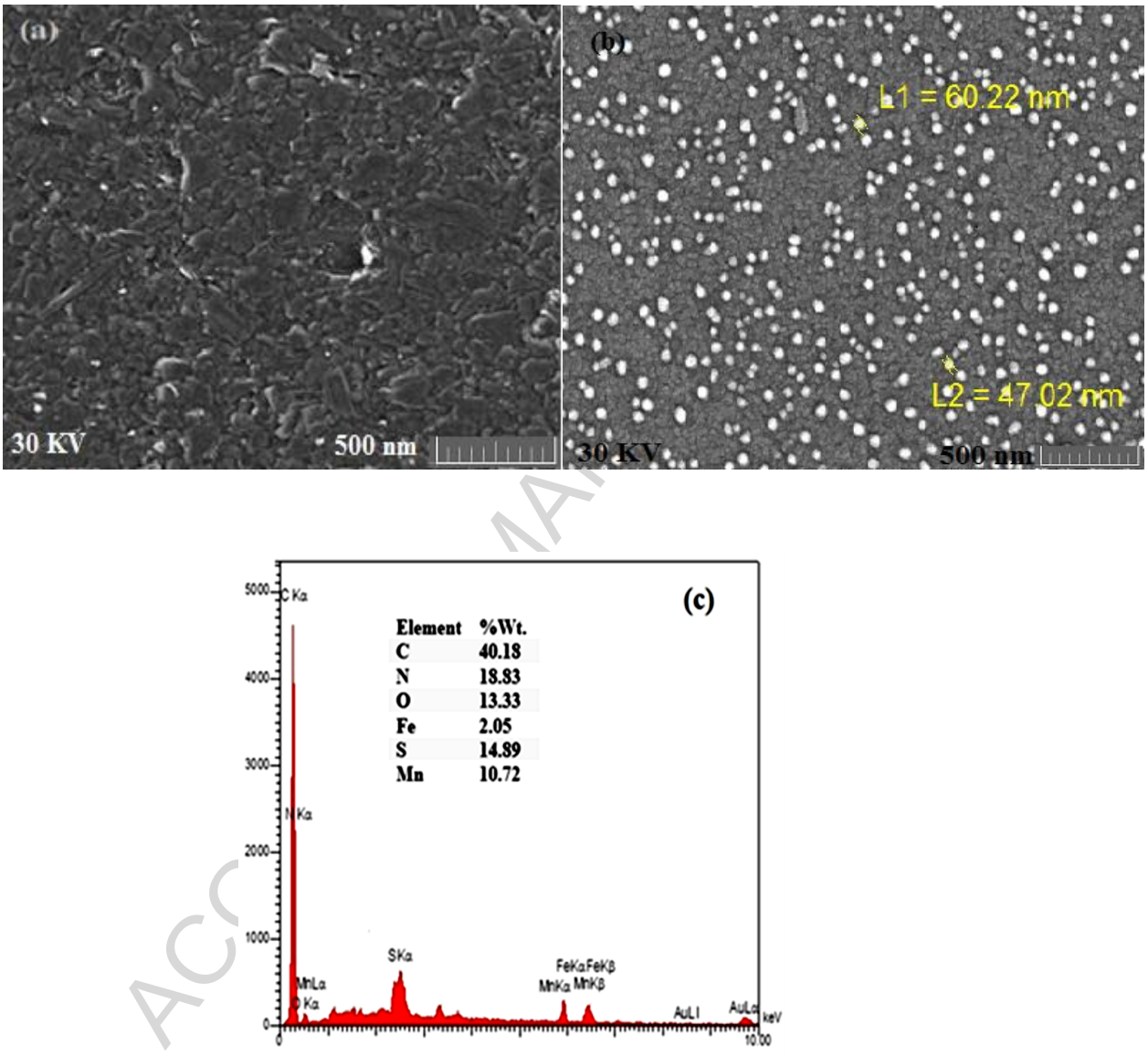

Figure 2

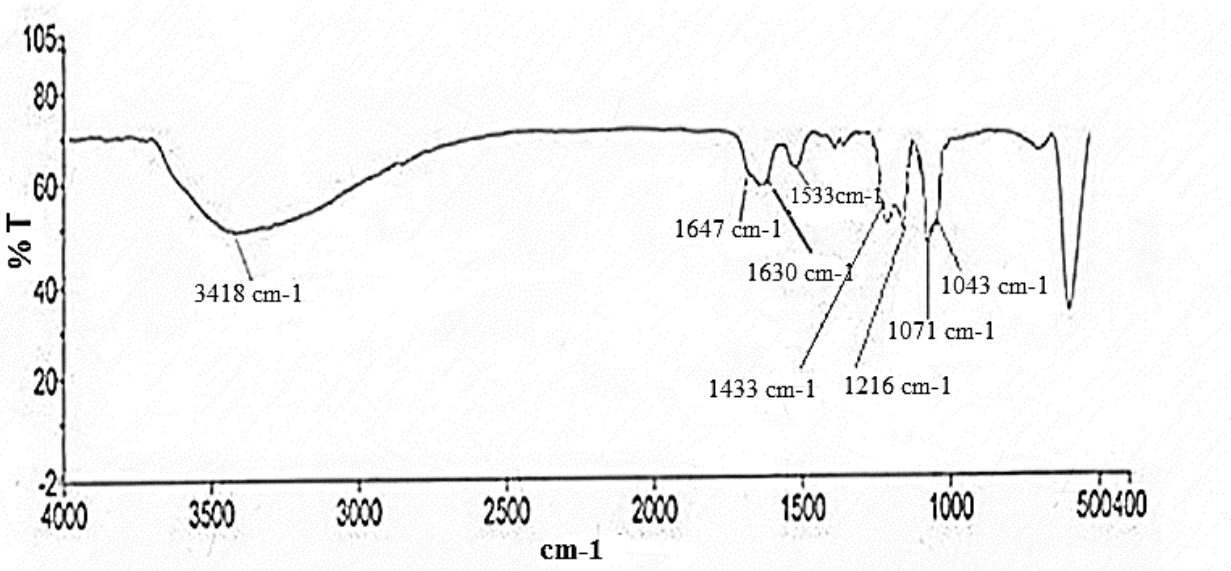

Figure 3

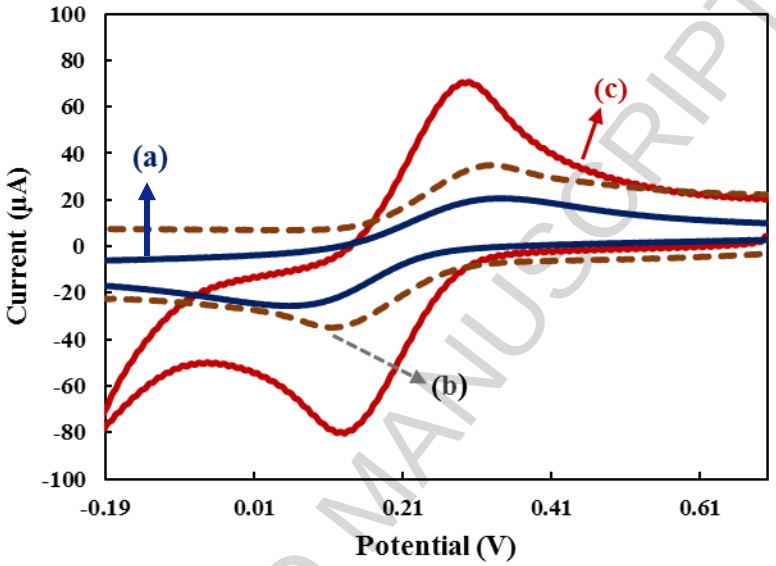

Figure 4

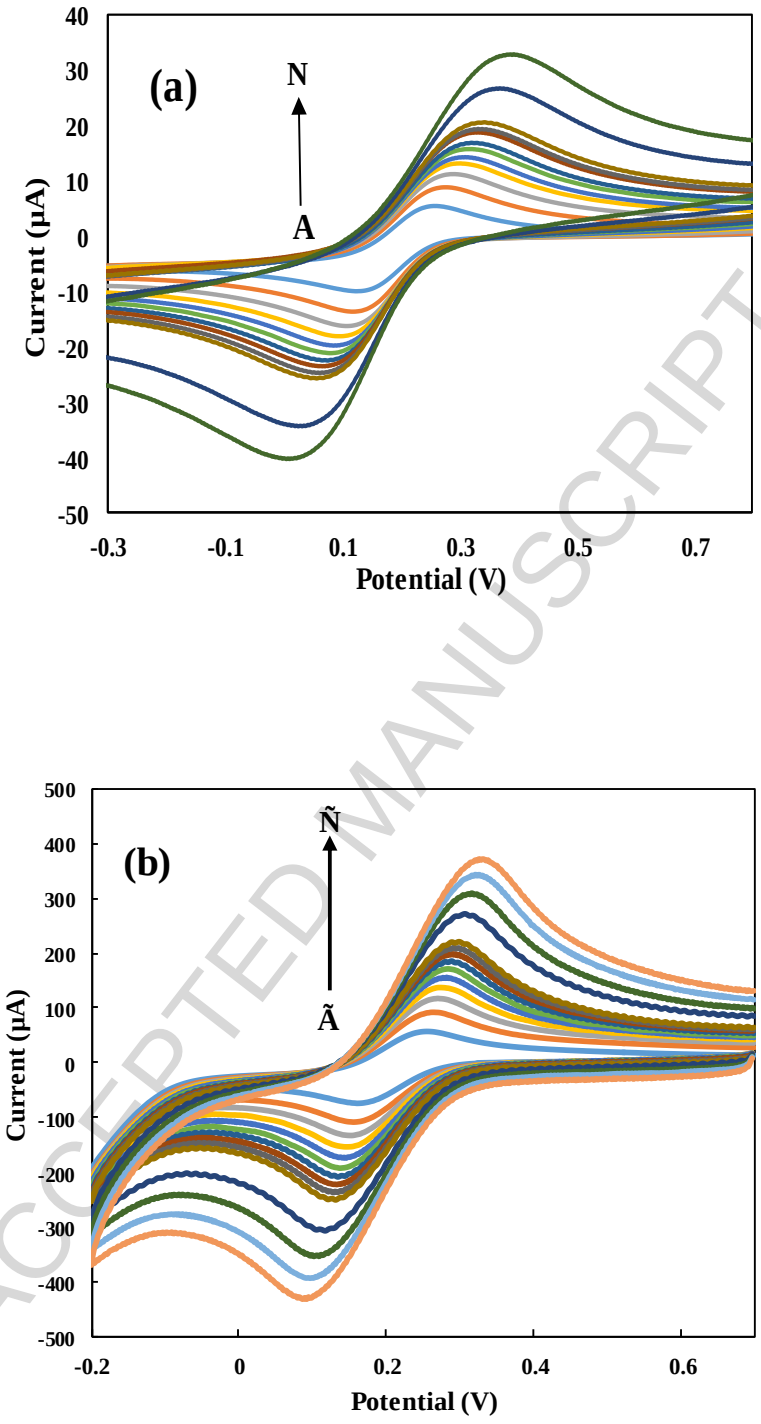

Figure 5

Figure 5 (Continue)

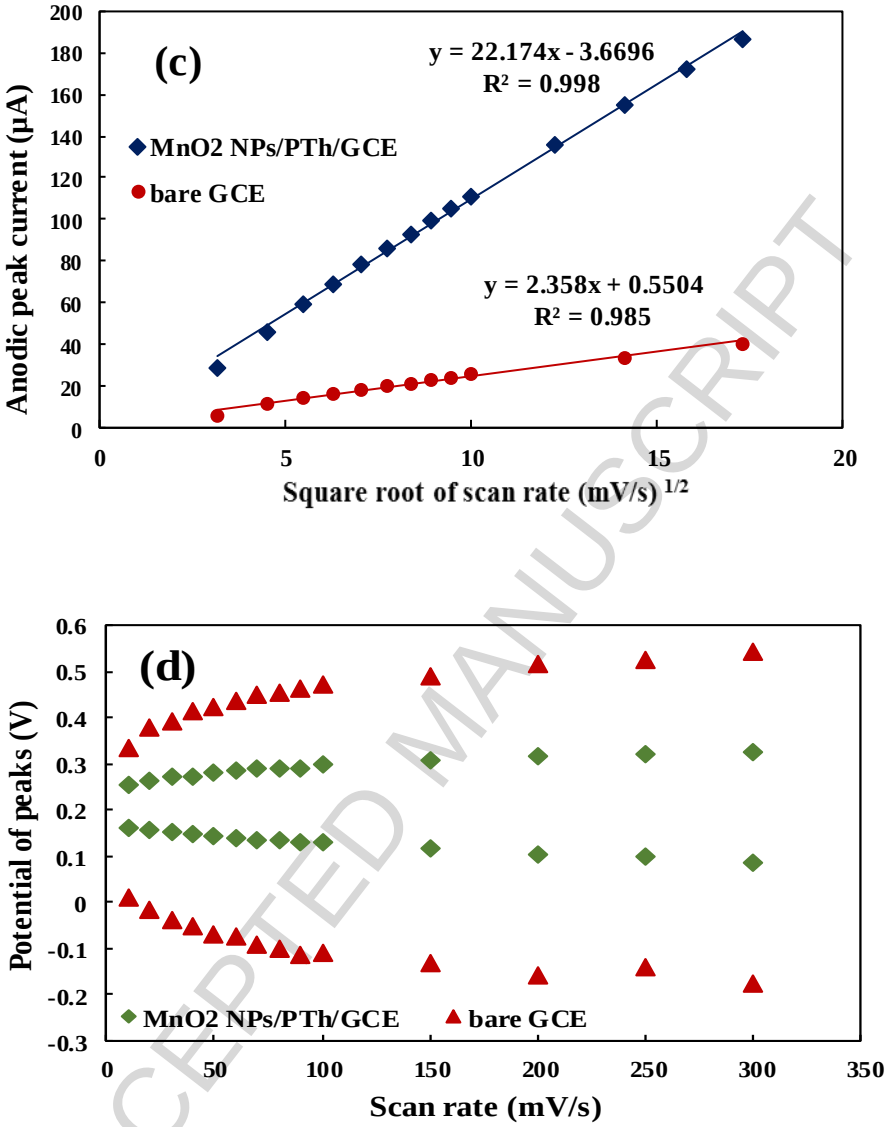

Figure 5

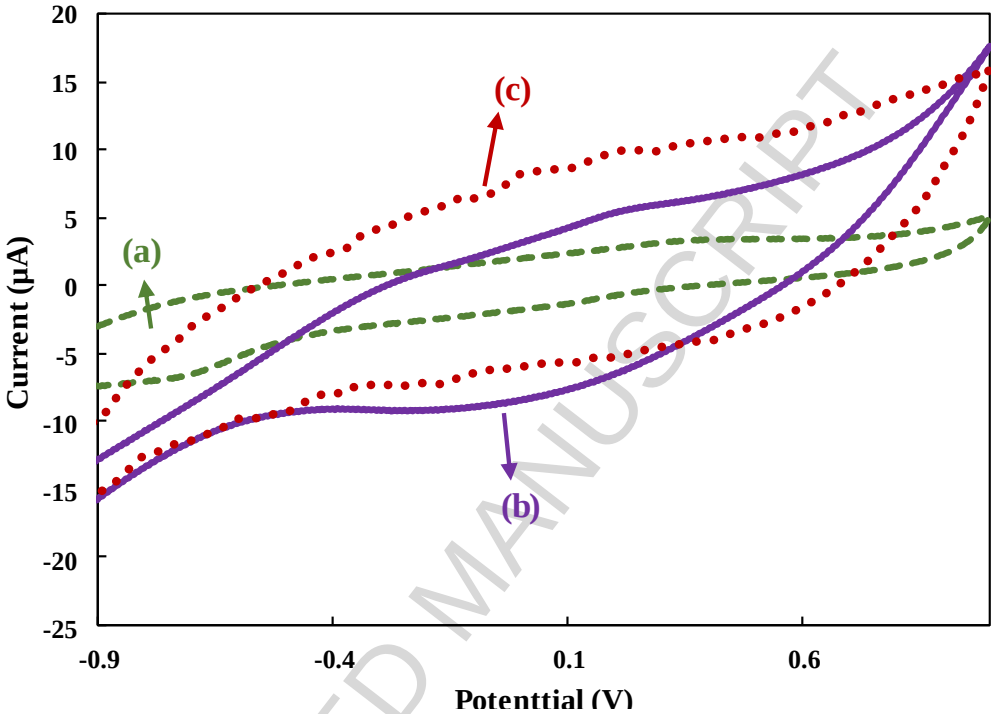

Figure 6

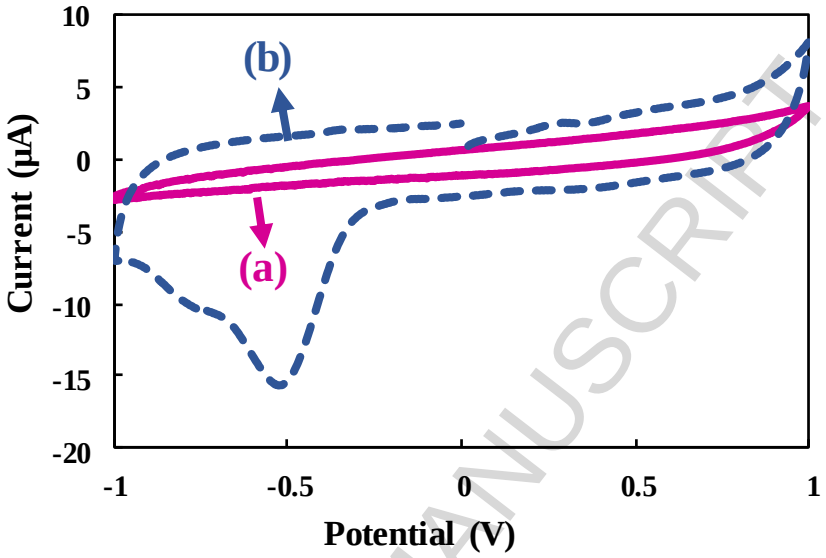

Figure 7

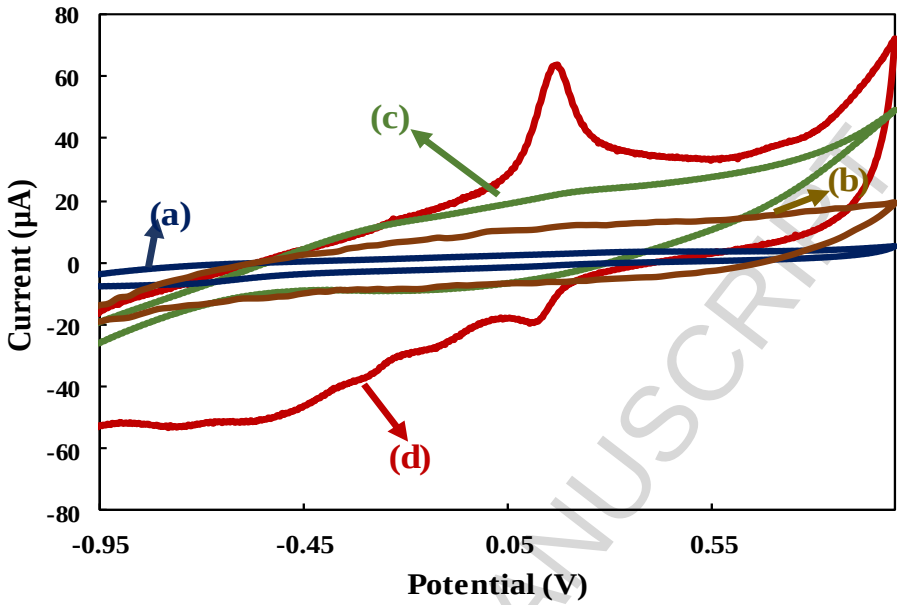

Figure 8

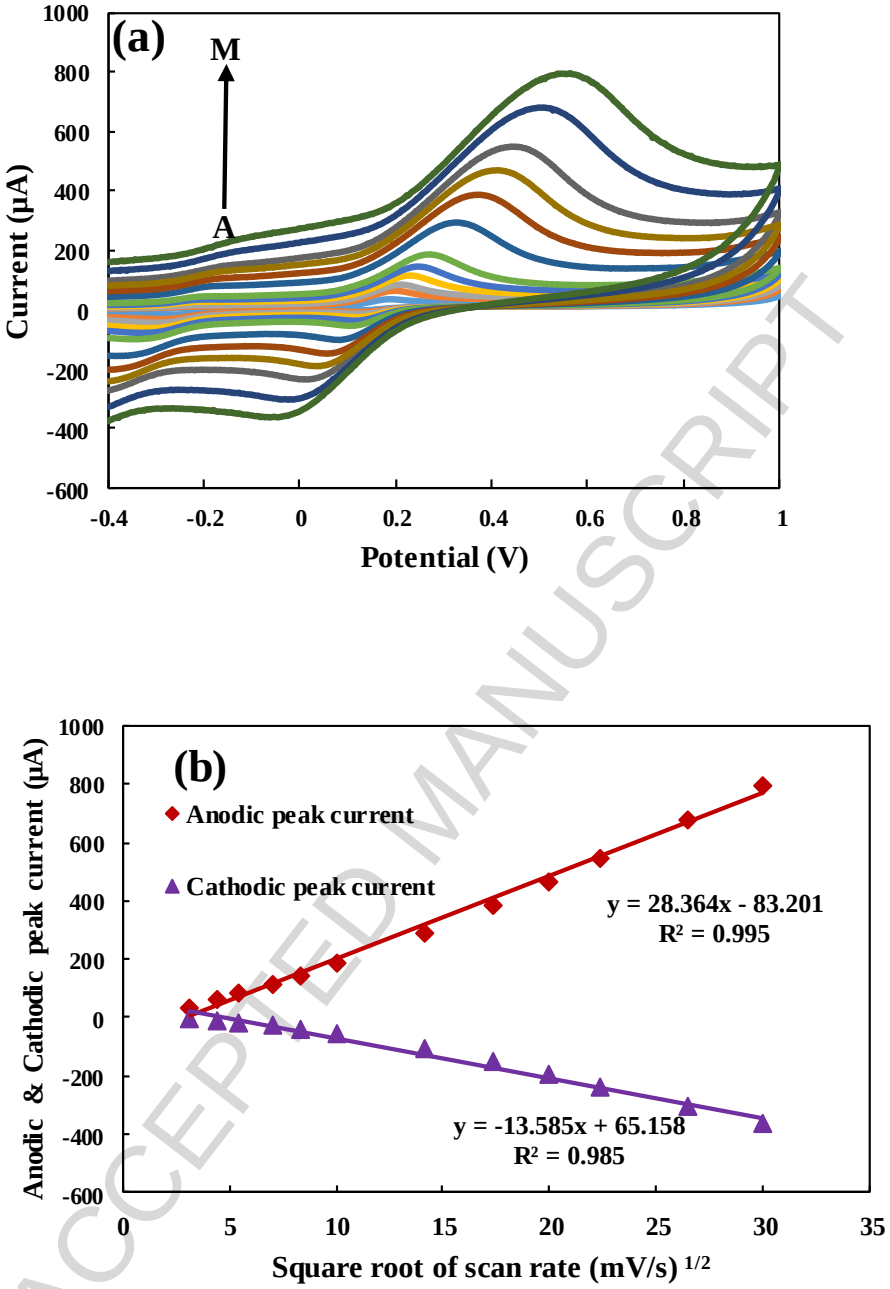

Figure 9

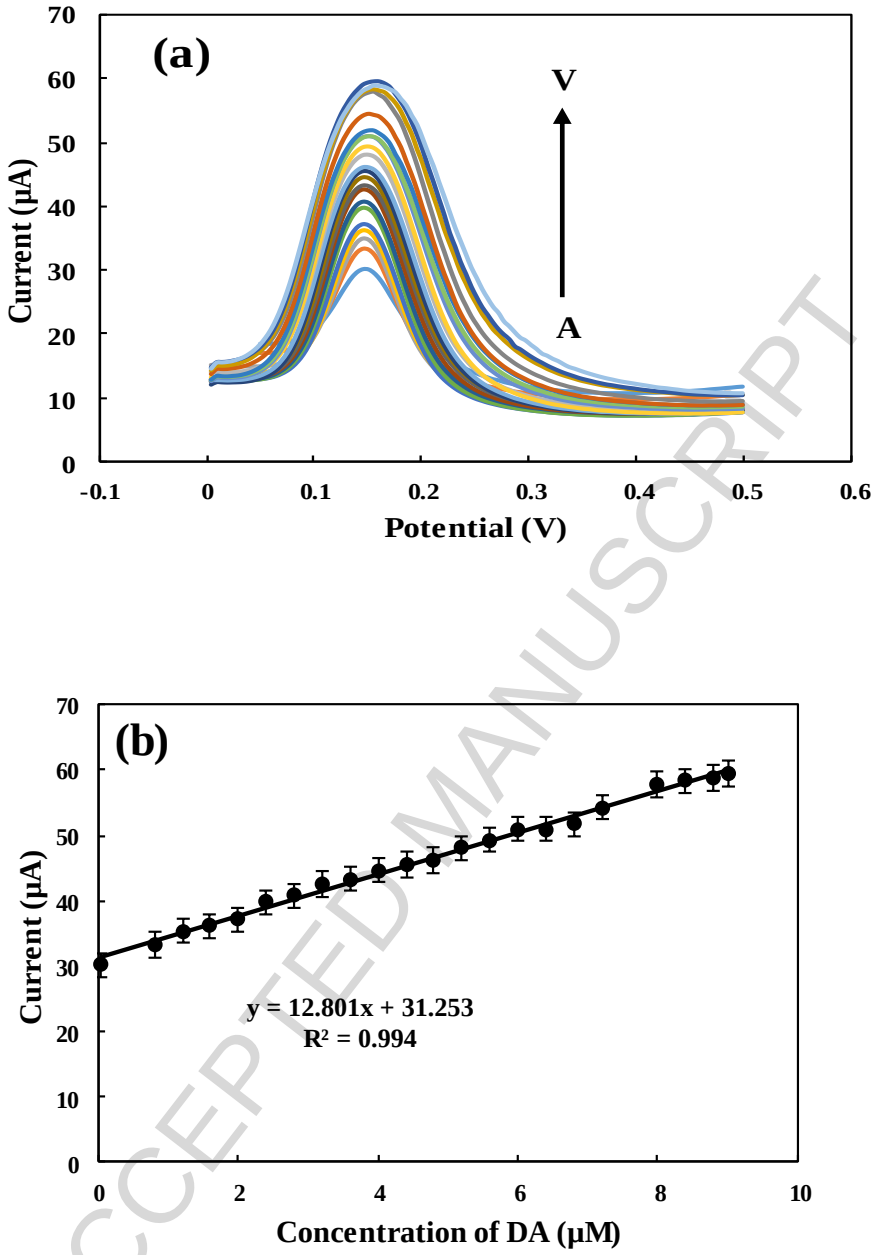

Figure 10

Figure 10 (continue)

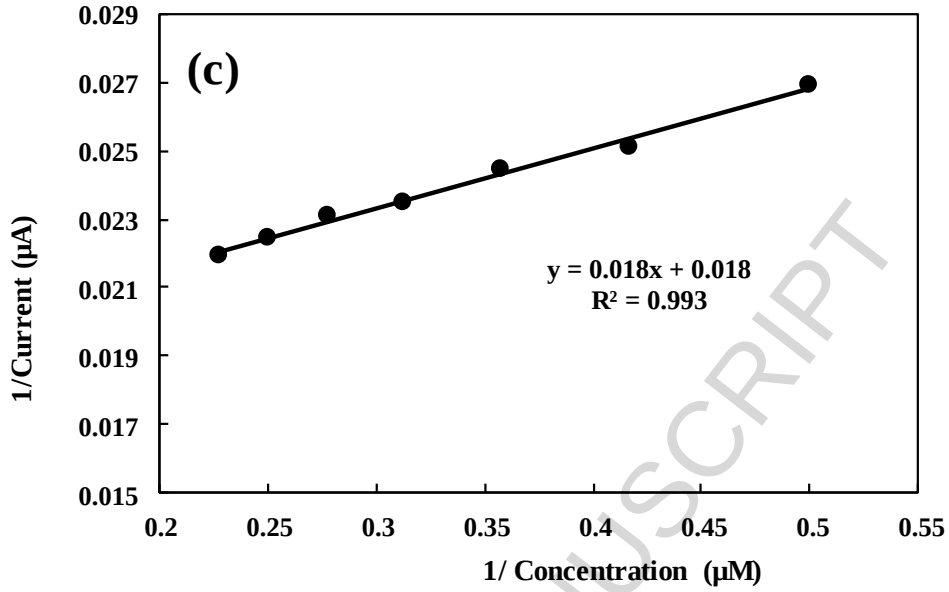

Figure 10

Polythiophene supported MnO_2 nanoparticles as nano-stabilizer for simultaneously electrostatically immobilization of D-amino acid oxidase and hemoglobin as efficient bio-nanocomposite in fabrication of dopamine bi-enzyme biosensor

Graphical Abstract

Research highlights:

✓ Novel bi-enzyme biosensor for determination of DA was fabricated by using D-alanine oxidation and developed in real samples.

✓ DAAO and Hb electrostatically immobilized at MnO_2 NPs which synthesized by soaking the PTh/GCE in potassium permanganate ($KMnO_4$) solution.

✓ Characterization of bi-enzyme biosensor was done by SEM, EDX and CV and the response of proposed biosensor was investigated by DPV and CV techniques.

✓ The modified biosensor showed good sensitivity, repeatability, stability and selectivity toward DA oxidation.